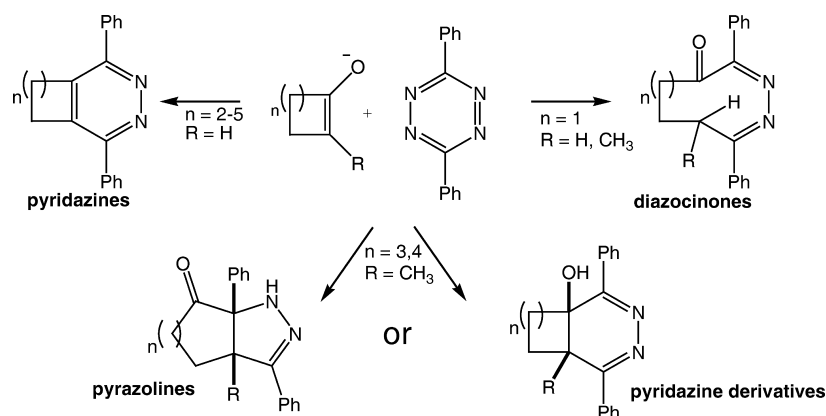# Mechanisms for Formation of Diazocinones, Pyridazines, and Pyrazolines from Tetrazines—Oxyanion-Accelerated Pericyclic Cascades?

Michael W. Lodewyk, Mark J. Kurth,* and Dean J. Tantillo*

Department of Chemistry, University of California, Davis, One Shields Avenue, Davis, California 95616

tantillo@chem.ucdavis.edu; kurth@chem.ucdavis.edu

Received March 13, 2009

A computational approach is utilized to study the diazocinone- and pyridazine-forming cascade reactions resulting from the reaction of 1,2,4,5-tetrazines with cyclic enolates. Many of the proposed reaction steps can be formulated as oxyanion-accelerated pericyclic processes. In examining these, a unique stepwise version of a formal (4 + 2) cycloaddition/(4 + 2) cycloreversion was discovered. For the key ring-opening step in these cascades, theoretical evidence for two distinct processes is reported. Of these two possibilities, an allowed six-electron electrocyclic ring-opening is predicted to be highly favored both kinetically and thermodynamically. Evidence for an unexpected oxyanion-accelerated 1,2-sigmatropic shift was also found for certain systems, leading to the theoretical prediction that seven- and eight-membered ring-fused pyrazoline systems could be formed experimentally under conditions similar to those for diazocinone and pyridazine formation.

Introduction

Symmetrical and unsymmetrical 1,2,4,5-tetrazines (herein referred to as tetrazines) have received much attention from the synthetic community for their usefulness as intermediates in natural product and pharmaceutical syntheses.[1] Their chemistry is dominated by their facile reactivity in inverse-electron-demand hetero-Diels—Alder reactions with various alkene and alkyne dienophiles. These cycloadditions are rapidly followed by N_2 extrusion (a retro-cycloaddition) to form substituted pyridazines directly (from alkynes) or dihydropyridazines (from alkenes), which may undergo further reactions to form pyridazines.[1]

Previous mechanistic studies on these cascade reactions have revealed numerous and sometimes unexpected details with regard to their kinetic parameters, stereo- and regioselectivities, and the roles of certain intermediates.[2] The details of these mechanisms appear to be highly system-dependent, however.

An unexpected route to 1,2-diazocinones (herein referred to as diazocinones) was uncovered two decades ago during the course of studies on the formation of pyridazines from tetrazines

(1) For reviews on the reactivity and applications of various tetrazines, see (a) Saracoglu, N. *Tetrahedron* **2007**, *63*, 4199–4236. (b) Boger, D. L. *Chem. Rev.* **1986**, *86*, 781–793.

(2) See for example: (a) Cioslowski, J.; Sauer, J.; Hetzenegger, J.; Karcher, T.; Hierstetter, T. *J. Am. Chem. Soc.* **1993**, *115*, 1353–1359. (b) Sauer, J.; Heldmann, D. K.; Hetzenegger, J.; Krauthan, J.; Sichert, H.; Schuster, J. *Eur. J. Org. Chem.* **1998**, 2885–2896. (c) Sadasivam, D. V.; Prasad, E.; Flowers, R. A., II. *J. Phys. Chem. A* **2006**, *110*, 1288–1294. (d) Hamasaki, A.; Ducray, R.; Boger, D. L. *J. Org. Chem.* **2006**, *71*, 185–193. (e) Hayden, A. E.; Houk, K. N. *J. Am. Chem. Soc.* **2009**, *131*, 4084–4089. (f) Domingo, L. R.; Picher, M. T.; Sáez, J. A. *J. Org. Chem.* **2009**, *74*, 2726–2735.

SCHEME 1
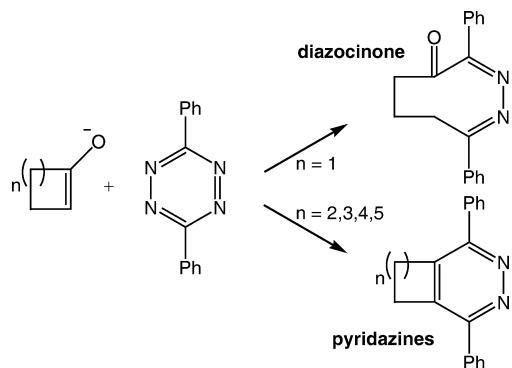
and various enolate species (Scheme 1).[3,4] A follow-up study then examined the conformational properties of several analogues of these systems.[5] These reactions, like the others mentioned above, are quite interesting from a mechanistic standpoint. While condensations of tetrazines with acyclic and five-, six-, seven-, and eight-membered ring enolates give the corresponding substituted pyridazines, condensation with an enolate derived from cyclobutanone gives the diazocinone instead.[3,4] Furthermore, several steps within these two pathways have the potential to occur via at least two possible mechanisms.

Scheme 2 highlights some of the mechanistic alternatives which are possible for these pyridazine- and diazocinone-forming reactions. The sequence begins with a (4 + 2) cycloaddition between the enolate and tetrazine, which may occur via either a concerted or (more likely) a stepwise process.[6] This cycloaddition is followed by the extrusion of nitrogen gas via a retro-cycloaddition reaction to give intermediate **4**. From here, several alternatives exist. If the enolate species is derived from a five-membered ring or larger, the reaction appears to follow an aromatization process via intermediate **5**, whereby H_2O is eliminated in order to form an aromatic system and yield the final fused pyridazine product.

However, if the enolate is derived from a cyclobutanone ($n = 1$), ring opening to form a diazocinone product occurs instead. One reasonable mechanistic proposal for this reaction is that intermediate **4** undergoes an oxyanion-accelerated six-electron, electrocyclic ring-opening reaction to give **6**,[7] which is then protonated at C7 to give the final product. Another reasonable proposal is that intermediate **4** fragments to form **7**, where a

carbonyl has formed as a delocalized carbanion is expelled. Whether or not **6** and **7** are distinct intermediates (perhaps conformers or geometric isomers) or simply canonical forms of the same resonance hybrid is not obvious.

In this study, we seek to address various questions related to Scheme 2 using a computational approach. Our results are presented in three parts: (1) the first two steps in the proposed mechanism (**1** + **2** → **3** → **4**) for which $n = 1$, (2) the ring-opening steps (**4** → **6** and/or **4** → **7**) for which $n = 1$, and (3) the behavior of systems for which $n > 1$.

Methods

All calculations were performed with the Gaussian03[8] software suite. Geometries were optimized without symmetry constraints using the B3LYP/6-31+G(d,p) method.[9,10] All stationary points were characterized as either minima or transition-state structures via frequency calculations, and the reported energies are computed free energies (including unscaled zero-point energy (ZPE) corrections). For several cases, the transition-state structures were linked to their corresponding minima via intrinsic reaction coordinate (IRC)[11] calculations (see Supporting Information for details). Anionic systems were generally treated without counterions.[12] Solvent optimization and single-point calculations in methanol were performed as indicated in the text at the same level of theory using the CPCM model and UAKS radii.[13] NICS(0)[14] calculations were performed at the B3LYP/6-311+G(2d,p)//B3LYP/6-31+G(d,p) level of theory. Electrostatic potential map images were created with Gaussian03 and GaussView; isovalues and potential ranges were used as indicated in the captions accompanying figures containing these images. Structural diagrams were produced using Ball & Stick version 4.0.[15]

Results and Discussion

Part 1: (4 + 2) Cycloaddition/(4 + 2) Cycloreversion. The first step shown in Schemes 2 and 3 involves the (4 + 2) cycloaddition of an enolate (**1**) and a diphenyl tetrazine (**2**). This process can be formulated as a concerted $[_\pi 4_s + _\pi 2_s]$ process as in the parent Diels−Alder reaction,[16] although the nature of

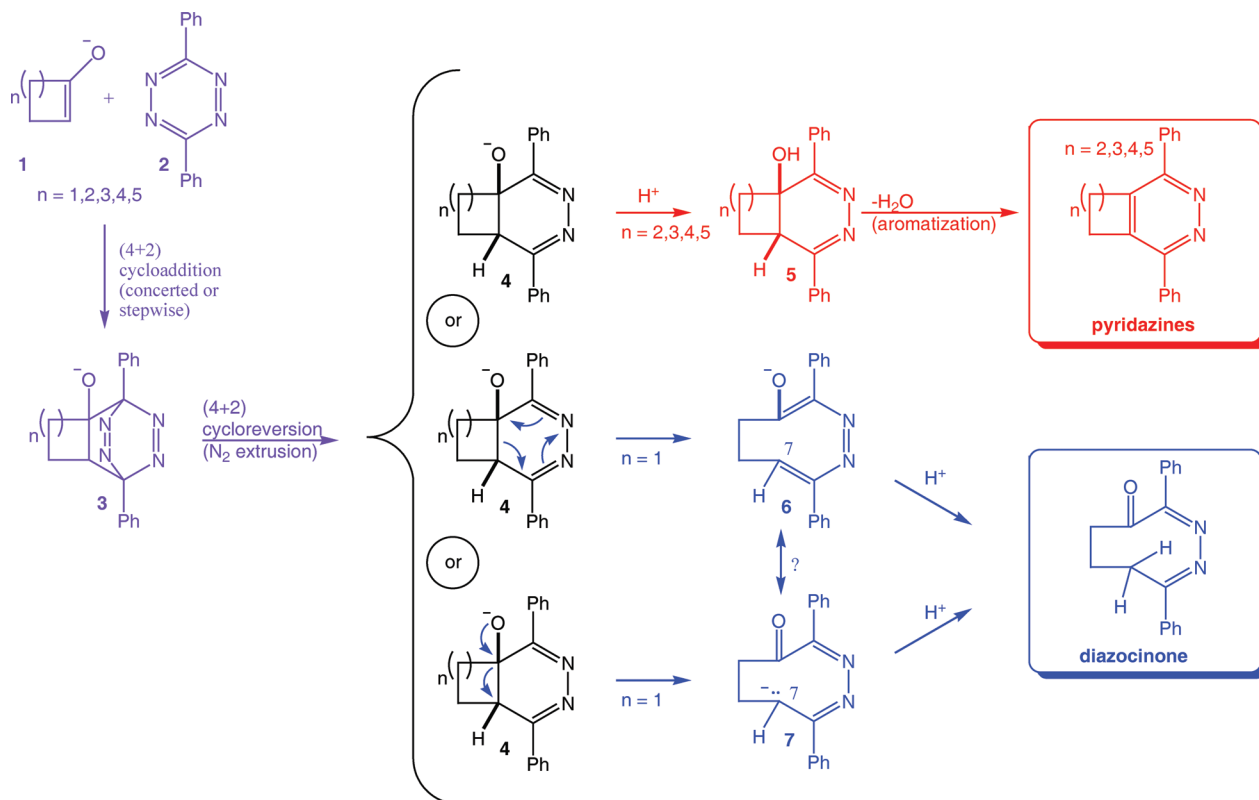(3) Haddadin, M. J.; Firsan, S. J.; Nader, B. S. *J. Org. Chem.* **1979**, *44*, 629–630.

(4) Haddadin, M. J.; Agha, B. J.; Salka, M. S. *Tetrahedron Lett.* **1984**, *25*, 2577–2580.

(5) Robins, L. I.; Carpenter, R. D.; Fettinger, J. C.; Haddadin, M. J.; Tinti, D. S.; Kurth, M. J. *J. Org. Chem.* **2006**, *71*, 2480–2485.
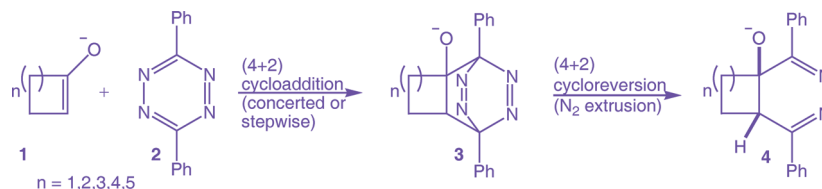
(6) Variations of these concerted cycloaddition reactions appear to lay along a continuum of synchronicity (see ref 2) but, in the case of anionic dienophiles, may be expected to proceed in a fully stepwise fashion with the formation of a distinct intermediate via initial nucleophilic attack of the enolate on the tetrazine. Indeed, this possibility has been previously proposed by Boger et al.[2] A related reaction is discussed in Camps, P.; Domingo, L. R.; Formosa, X.; Galdeano, C.; González, D.; Muñoz-Torrero, D.; Segalés, S.; Font-Bardia, M.; Solans, X. *J. Org. Chem.* **2006**, *71*, 3464–3471.

(7) For reviews and leading references which discuss other oxyanion-accelerated pericyclic processes, see (a) Paquette, L. A.; Liu, Z.; Ramsey, C.; Gallucci, J. C. *J. Org. Chem.* **2005**, *70*, 8154–8161. (b) Kim, S.-H.; Cho, S. Y.; Cha, J. K. *Tetrahedron* **2001**, *42*, 8769–8772. (c) Wilson, S. R. In *Organic Reactions*; Paquette, L. A., Ed.; John Wiley & Sons, Inc.: New York, 1993; Vol. 43, pp 93. (d) Bronson, J. J.; Danheiser, R. L. In *Comprehensive Organic Synthesis*; Trost, B. M., Fleming, I., Eds.; Pergamon: Oxford, 1991; Vol. 5, pp 999−1035. (e) Zoeckler, M. T.; Carpenter, B. K. *J. Am. Chem. Soc.* **1981**, *103*, 7661−7663. (f) Paquette, L. A. *Tetrahedron* **1997**, *53*, 13971−14020. (g) Bunnage, M. E.; Nicolaou, K. C. *Chem.−Eur. J.* **1997**, *3*, 187−192.

(8) Frisch, M. J. *Gaussian03*, revision D.01; Gaussian, Inc.: Pittsburgh, PA, 2003 (full reference in Supporting Information).

(9) (a) Becke, A. D. *J. Chem. Phys.* **1993**, *98*, 5648–5652. (b) Becke, A. D. *J. Chem. Phys.* **1993**, *98*, 1372–1377. (c) Lee, C.; Yang, W.; Parr, R. G. *Phys. Rev. B* **1988**, *37*, 785–789. (d) Stephens, P. J.; Devlin, F. J.; Chabalowski, C. F.; Frisch, M. J. *J. Phys. Chem.* **1994**, *98*, 11623–11627. (e) The value of diffuse functions in density functional based calculations was recently discussed in Lynch, B. J.; Zhao, Y.; Truhlar, D. G. *J. Phys. Chem. A* **2003**, *107*, 1384–1388.

(10) For recent papers involving computations on enolate structures with B3LYP methods, see (a) Pratt, L. M.; Nguyen, S. C.; Thanh, B. T. *J. Org. Chem.* **2008**, *73*, 6086–6091. (b) Domingo, L. R.; Arnó, M.; Merino, P.; Tejero, T. *Eur. J. Org. Chem.* **2006**, 3464–3472. (c) Zhang, X.; Houk, K. N. *J. Org. Chem.* **2005**, *70*, 9712–9716. (d) Pratt, L. M.; Nguyen, N. V.; Ramachandran, B. *J. Org. Chem.* **2005**, *70*, 4279–4283.

(11) (a) Gonzalez, C.; Schlegel, H. B. *J. Phys. Chem.* **1990**, *94*, 5523–5527. (b) Fukui, K. *Acc. Chem. Res.* **1981**, *14*, 363–368. (c) IRC plots are available in the Supporting Information.

(12) With the inclusion of a potassium counterion on smaller model systems, energies for the transition-state structures and products were raised relative to the reactants; however, these numbers are not highly reliable due to the tendency of this counterion to interact with various electron-rich atoms in the structures and the presence of several conformers of these systems.

(13) (a) Barone, V.; Cossi, M. *J. Phys. Chem. A* **1998**, *102*, 1995–2001. (b) Barone, V.; Cossi, M.; Tomasi, J. *J. Comput. Chem.* **1998**, *19*, 404–417. (c) Takano, Y.; Houk, K. N. *J. Chem. Theory Comput.* **2005**, *1*, 70–77.

(14) For leading references, see (a) Schleyer, P. v. R.; Maerker, C.; Dransfeld, A.; Jiao, H.; Hommes, N. J. R. v. E. *J. Am. Chem. Soc.* **1996**, *118*, 6317–6318. (b) Chen, Z.; Wannere, C. S.; Corminboeuf, C.; Puchta, R.; Schleyer, P. v. R. *Chem. Rev.* **2005**, *105*, 3842–3888.

(15) Müller, N.; Falk, A.; Gsaller, G. *Ball & Stick* version 4.0a12, molecular graphics application for MacOS computers; Johannes Kepler University: Linz, 2004.

SCHEME 2

SCHEME 3

the reactants (the diene is very electron-poor and the dienophile very electron-rich) suggests that an alternative stepwise process may be at play.[6] Shown in Figure 1 for $n = 1$ is the first stationary point we located involving both reactants ($\mathbf{1} + \mathbf{2}$ complex). Because it exhibits a single imaginary frequency (-31.94 cm^{-1}) corresponding to a vibration in which the enolate carbon moves between the two tetrazine carbon atoms, this structure is a transition-state structure. IRC calculations from this structure failed to find an associated minimum, which is consistent with this region of the potential energy surface being rather flat, as implied by the small magnitude of the imaginary frequency. A scan in which the distance between the enolate carbon atom and one carbon atom in the tetrazine was gradually reduced (see Supporting Information) revealed no energy barrier between the $\mathbf{1} + \mathbf{2}$ complex and structure $\mathbf{3'}$, which is more than 10 kcal/mol lower in energy than the complex. The presence of structure $\mathbf{3'}$, which lacks a full bond between C3 and C4, and the ease with which it is formed from the $\mathbf{1} + \mathbf{2}$ complex strongly suggest that a concerted [4 + 2] cycloaddition

does not occur. Additionally, explicit attempts (including the use of various constrained calculations) to find a concerted transition-state structure failed.

As mentioned above, $\mathbf{3'}$ in Figure 1 does not exactly correspond to $\mathbf{3}$ in Schemes 2 and 3. With a C3–C4 distance of 2.8 Å, $\mathbf{3'}$ appears to be an intermediate along the stepwise pathway to $\mathbf{3}$ that is preorganized for subsequent ring closure. Nonetheless, no closed-form intermediate corresponding to $\mathbf{3}$ in Schemes 2 and 3 could be found.[17] Instead, $\mathbf{3'}$ was found to be connected (through an IRC calculation, see Supporting Information) to a transition-state structure for N$_2$ extrusion leading to structure $\mathbf{4}$. In other words, the C3–C4 bond forms as N$_2$ leaves. These events occur rather asynchronously;[18] in the transition-state structure, the C–C bond is mostly formed (1.70 Å) while the two C–N bonds are only partially broken (1.68 and 1.93 Å). Note that the overall situation here with an enolate dienophile is somewhat different than that described very recently by Domingo et al.,[2f] where an enamine dienophile was found to form a cycloadduct analogous to structure $\mathbf{3}$ with an

(16) (a) Woodward, R. B.; Hoffmann, R. *The Conservation of Orbital Symmetry*; Verlag Chemie: Weinheim, Germany, 1970. (b) Hoffmann, R.; Woodward, R. B. *Acc. Chem. Res.* **1968**, *1*, 17–22, and references therein. (c) Woodward, R. B.; Hoffmann, R. *Angew. Chem., Int. Ed. Engl.* **1969**, *8*, 781–853.

(17) Efforts here included constrained calculations and a relaxed potential energy surface scan (see Supporting Information) where the C3–C4 distance was gradually decreased. This scan revealed no energetic well down to 1.4 Å.

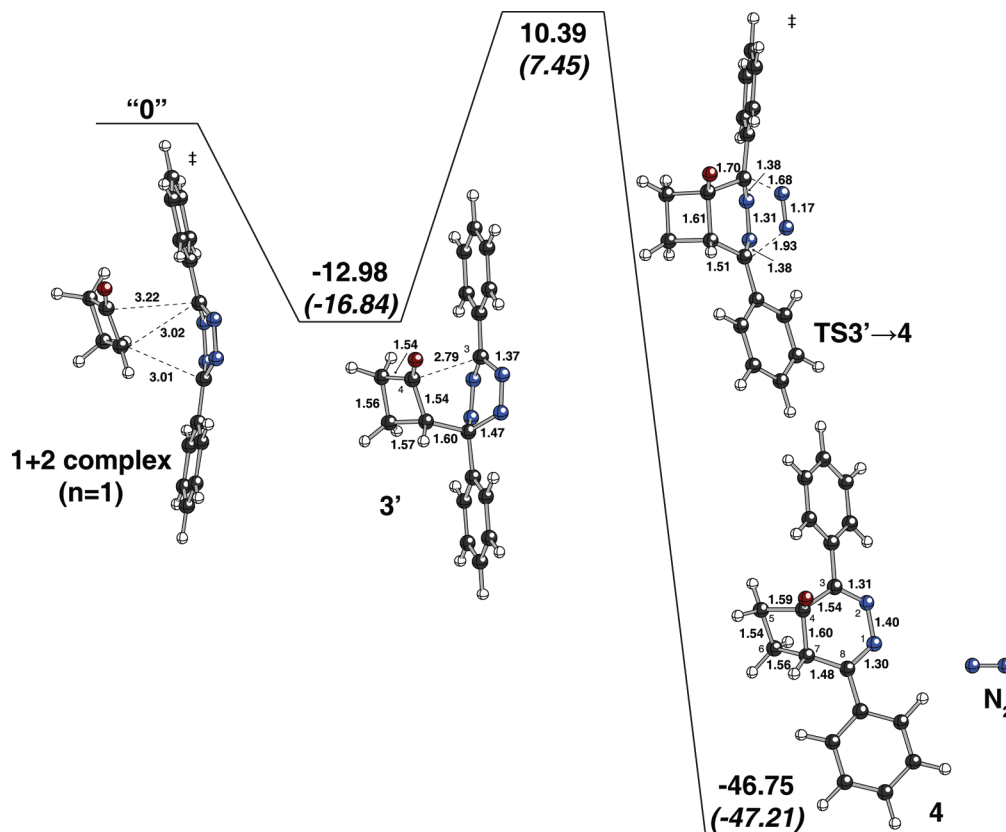(18) Tantillo, D. J. *J. Phys. Org. Chem.* **2008**, *21*, 561–570.

FIGURE 1. Computed geometries and energies (B3LYP/6-31+G(d,p)) for stationary point structures involved in the transformation of the **1 + 2** complex to **4** + N_2 ($n = 1$). Energies are in kcal/mol; regular text shows gas-phase free energy values; italicized text in parentheses shows solvent single-point electronic energy values (see Methods). Selected distances are in Å.

SCHEME 4

SCHEME 5
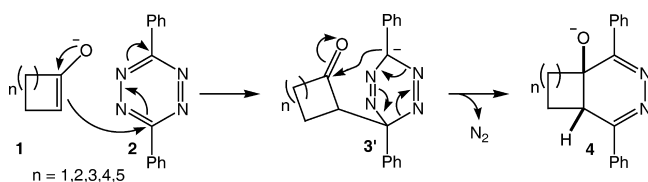
unsymmetrically substituted tetrazine, providing further evidence that mechanistic details such as these are highly system-dependent.

Reaction **3′ → 4** has an energy barrier of 23−24 kcal/mol from structure **3′**, and the resulting intermediates (**4** + N_2) are approximately 47 kcal/mol lower in energy than the **1 + 2** complex. Therefore, we suggest that the cycloaddition and cycloreversion steps do not occur separately, with the two C−C bonds first being formed, followed by the two C−N bonds breaking (Schemes 2 and 3), but instead occur in a different fashion, where the first step involves formation of one C−C bond with the other three bond-making/breaking events occurring in a concerted but asynchronous manner in the second step (Scheme 4).[18,19]

Part 2: Ring-Opening Possibilities. On the surface, it may appear that structures **6** and **7** (Schemes 2 and 5) represent the same chemical species and are merely resonance forms of the same structure. On the other hand, the processes (see arrows)
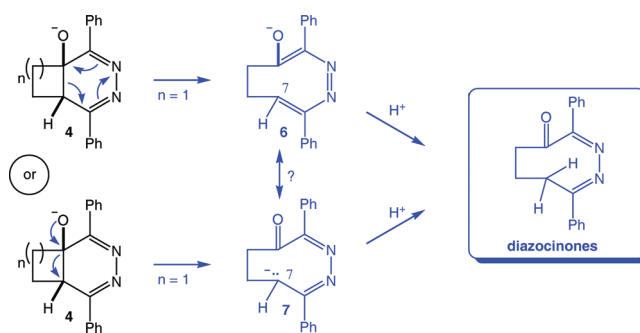
by which intermediate **4** leads to **6** and **7** appear to be different from each other. Whether or not these two possibilities are actually distinct and are both viable is one of the key questions of this study, a question we initially approached with a search for transition-state structures for both processes.

Figure 2 shows two transition-state structures that we were able to locate (**TS4 → 6**, and **TS4 → 7**). It is obvious that these structures do differ significantly from each other (both structurally and energetically), yet examination of the imaginary frequencies associated with each of these structures suggests that they do indeed both correspond to ring-opening processes. In fact, IRC calculations (see Supporting Information) connect each structure to a single common reactant in the reverse direction but to two different products (**6** and **7**) in the forward direction (Figure 2).

Several features of the structures shown in Figure 2 are worth noting. First, **TS4 → 6** appears to correspond to a six-electron electrocyclic ring-opening reaction. As expected based on orbital

(19) Although not exactly the same, this situation bears resemblance to so-called "bis-pericyclic" reactions, where two cycloadditions are merged into a single process. For leading references and a discussion of these and other hybrid pericyclic reactions, see Nouri, D. H.; Tantillo, D. J. *J. Org. Chem.* **2006**, *71*, 3686–3695.
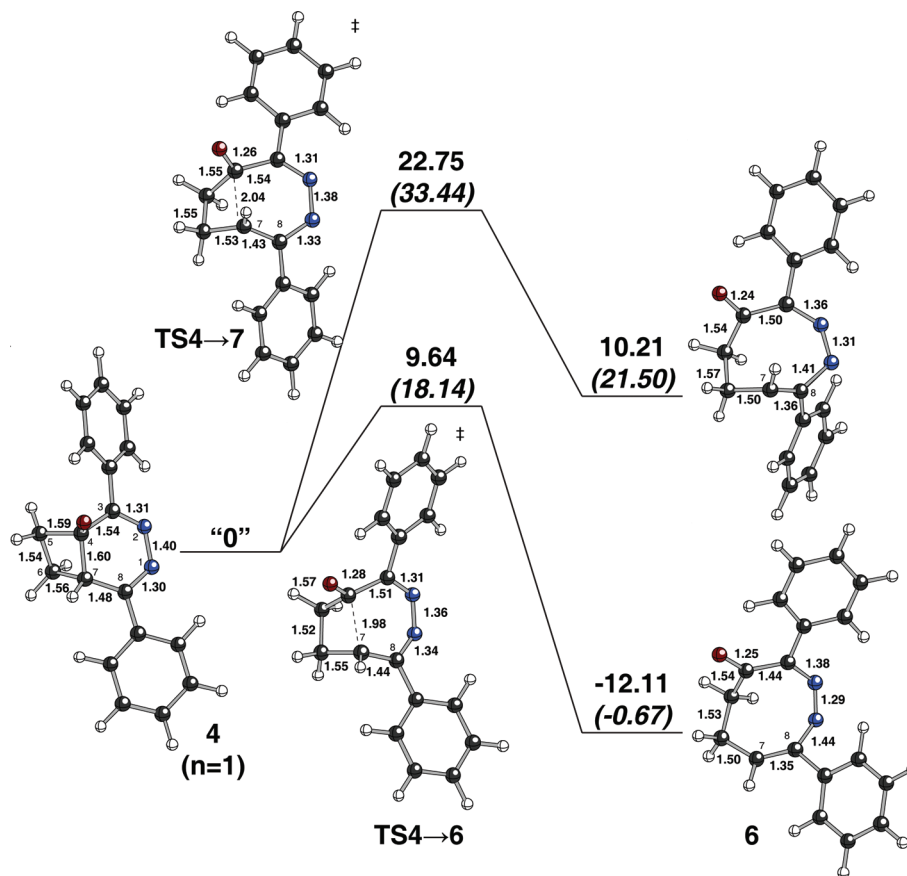
FIGURE 2. Computed geometries and energies (B3LYP/6-31+G(d,p)) for stationary point structures involved in the transformation of **4** to **6** and **4** to **7** ($n = 1$). Energies are in kcal/mol; regular text shows gas-phase free energy values; italicized text in parentheses shows solvent single-point electronic energy values (see Methods). Selected distances are in Å.

symmetry considerations,[16] product **6** appears to result from net disrotation of the oxygen atom and hydrogen atom connected to C7; in this case, both atoms have rotated outward.[20] Furthermore, a NICS(0) calculation for this transition-state structure yields a value of −4.5 ppm, suggesting that it possesses some aromatic character.[14,21]

In contrast, **TS4 → 7** represents an alternative ring-opening process whereby a delocalized carbanion is expelled from an incipient carbonyl group. This process resembles both a Grob fragmentation[22] and a retro-aldol process and is perhaps best categorized as nonpericyclic. Interestingly though, while the ring-opened product **7** (Figure 2) again has the oxygen atom rotated toward the outside of the ring, the hydrogen atom on C7 has rotated toward the inside of the ring. Together, these two motions correspond to net conrotation.[20] Furthermore, a computed NICS(0) value of +4.1 suggests

that **TS4 → 7** may possess some antiaromatic character, as expected for an orbital symmetry-forbidden process.[23] In reality, it appears that the process lies somewhere between nonpericyclic and forbidden pericyclic. Not surprisingly, the process leading to the orbital symmetry-allowed electrocyclic product is highly favored over this alternative. This preference correlates with the difference in aromaticity of the two transition-state structures, and in addition, the **4 → 6** reaction leads to a lower energy configuration of the product (note the Z configuration about C7−C8 in **6**, and the E configuration about C7−C8 in **7**). The difference in strain energy between these two products is partially manifested in the transition-state structures leading to them.
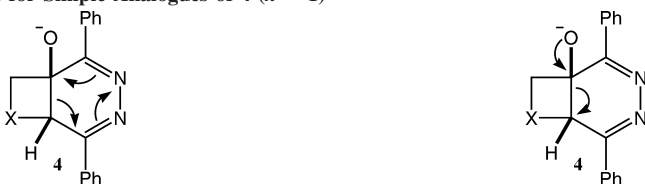
On the basis of these results, we can predict with some confidence that, while both processes could occur at room temperature or in refluxing methanol (conditions used experimentally[3−5]), this reaction likely follows the allowed electrocyclic alternative exclusively (for $n = 1$). However, note that finding experimental evidence in support of this contention is quite challenging given that the next step in the reaction involves protonation at C7, a

(20) One would expect that the vibrations corresponding to the imaginary frequencies of the transition structures leading to the disrotatory and conrotatory products would display these same motions upon animation. However, the situation appears to be complicated by the strongly interacting oxygen atom. While the hydrogen atom on C7 clearly rotates outwards in **TS4 → 6**, and clearly rotates inwards in **TS4 → 7**, the movement of the oxygen atom appears to correspond primarily to planarization of the carbon center in both animations. That is, the oxygen atom does not appear to rotate in a clear sense in either case. See Supporting Information for additional discussion and details including animated movies of imaginary frequencies. For a related ring-opening process, see Polo, V.; Domingo, L. R.; Andrés, J. *J. Org. Chem.* **2006**, *71*, 754–762.

(21) Benzene at the same level of theory has a NICS(0) value of −7.7, and the parent six-electron electrocyclization (hexatriene → cyclohexadiene) has a NICS(0) value of −13.4 ppm.

(22) Grob, C. A. *Angew. Chem., Int. Ed. Engl.* **1969**, *8*, 535–622.

(23) (a) The parent all-carbon six-electron electrocyclic orbital symmetry-forbidden conrotatory ring-opening reaction (1,3-cyclohexadiene → 1,3,5-hexatriene) has a computed reaction barrier of 57.5 kcal/mol (UB3LYP/6-31+G(d,p)) and a computed NICS(0) value of +21.9 (UB3LYP/6-311+G(2d,p)//(UB3LYP/6-31+G(d,p)). The same structure computed with a restricted closed shell configuration was found to have an RHF→UHF instability. (b) For other recent examples where orbital symmetry-forbidden transition structures have been computed, see De Proft, F.; Chattaraj, P. K.; Ayers, P. W.; Torrent-Sucarrat, M.; Elango, M.; Subramanian, V.; Giri, S.; Geerlings, P. *J. Chem. Theory Comput.* **2008**, *4*, 595−602; Sakai, S. *J. Phys. Chem. A* **2006**, *110*, 6339–6344.

TABLE 1.   Ring-Opening Reactions for Simple Analogues of 4 (*n* = 1)[a]

X	allowed electrocyclic		fragmentation	
	$\Delta E^{\ddagger}$	ΔE	$\Delta E^{\ddagger}$	ΔE
CH$_2$	9.64 *(18.14)*	−12.11 *(−0.67)*	22.75 *(33.44)*	10.21 *(21.50)*
O	5.36 *(10.29)*	−8.60 *(5.12)*	26.61 *(37.60)*	13.09 *(25.29)*
S	8.99 *(16.98)*	−1.75 *(9.94)*	26.68 *(36.12)*	13.07 *(25.60)*
NH	4.03 *(9.42)*	−11.97 *(0.71)*	22.56 *(35.12)*	7.42 *(19.19)*

[a] Energies (B3LYP/6-31+G(d,p)) are in kcal/mol; regular text shows gas-phase free energy values, and italicized text in parentheses shows solvent single-point electronic energy values (see Methods).
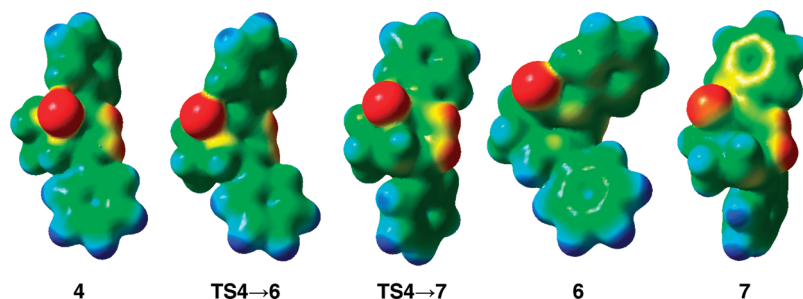

FIGURE 3. Electrostatic potential surfaces for structures shown in Figure 2 (see Methods section; isovalue = 0.01, potential range = −0.20 (red) to 0.00 (blue)).

step that would produce different conformers of the same product (rather than isomers) regardless of whether **6** or **7** is involved.[24]

We were, however, intrigued by the possibility of observing a product that would result from a formally forbidden electrocyclic reaction and wondered whether the inherent preference for the electrocyclic process could be altered through substituent effects. We began our search here with simple, synthetically accessible analogues of the cyclobutanone system. Specifically, we considered analogues where C3 in the cyclobutanone (C6 in Figure 2) is replaced with oxygen, sulfur, and NH groups. However, as shown in Table 1, the barrier for the allowed electrocyclic process was, in each case, lowered, and the barrier for the fragmentation process was raised relative to those for the system in Figure 2 (X = CH$_2$ in Table 1). We also considered placing an electron-withdrawing group at or near C7, reasoning that the higher energy pathway may result in a

buildup of electron density near C7 relative to the reactant as suggested by the arrows for this process (and by electrostatic potential maps for model systems lacking the phenyl rings; see Supporting Information). To our surprise, the analogue with both phenyl groups replaced by *p*-cyanophenyl groups (and X = CH$_2$) displayed almost no change for the relative barriers for the two competing processes (8.77 and 22.23 kcal/mol). This prompted an examination of electrostatic potential maps for the parent structures (Figure 3; structures oriented as in Figure 2), which suggest that there is not a significant buildup of electron density near C7 of **TS4 → 7** relative to **TS4 → 6**. Other attempts to place electron-withdrawing groups near C7 also either did not change the preference for the electrocyclic alternative or did not result in optimized transition-state structures for the two processes of interest.[25]

Part 3: Larger Systems. We also explored the behavior of systems for which *n* > 1, which are known experimentally to form pyridazines (Schemes 2 and 6).[26] Specifically, we wanted to determine whether blocking the aromatization pathway would allow ring opening to form systems with nine-membered and larger rings.[27]

We began with a search for the ring-opening transition-state structures for analogues of **4** derived from cyclopentanone through cyclooctanone (*n* = 2−5, Schemes 2 and 6) and soon encountered an unexpected result. For the cyclohexanone- and

---

(24) As delineated in the scheme below (adapted from the Ph.D. dissertation of Richard Carpenter, UC Davis, 2008), NMR-monitored reaction of bisphenyl tetrazine with a silylenolether analogue of **1** (*n* = 1), followed by treatment with TMSCl, led exclusively to product B, as evidenced by the presence of an alkene proton signal at 4.6 ppm in the ^{1}H NMR spectrum and the absence of a ketone carbonyl in the ^{13}C NMR spectrum. The absence of TMS-trapped product A is consistent with an analogue of **6**, rather than **7** occurring along the pathway to the diazocinone product for this particular system, although TMS migration (inter- or intramolecularly) cannot be ruled out.
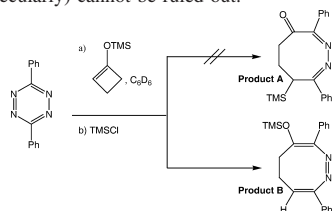
(25) These attempts included placing a phenyl group directly on C7, a CN group directly on C7, and CN groups directly on C3 and C8 (the tetrazine carbons). See Supporting Information for the structures we were able to locate and the corresponding energies.

(26) The discussion here will be limited to the ring-opening pathways that are potentially available to these systems. For results related to the pyridazine-forming steps themselves (i.e., protonation and elimination of water), see the Supporting Information.

SCHEME 6
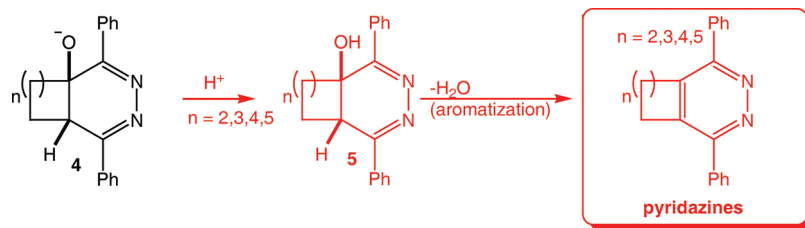
cycloheptanone-derived systems, we found the structures shown in Figure 4 instead of the expected electrocyclic ring-opening transition-state structures. These new structures correspond to oxyanion-accelerated [1s, 2s]-sigmatropic shifts to produce 7,5- and 8,5-fused ring systems.

Note that, with barriers of up to 35 kcal/mol, these two reactions are not predicted to be facile at or near room temperature, although they are significantly exergonic. The fact that they have not been observed experimentally[3−5] further points to the likelihood that the aromatization pathway is kinetically favored and is likely exergonic, as well.

Table 2 shows the computed barriers and reaction energies for the electrocyclic (or 1,2-shift) and fragmentation pathways for various systems (see Supporting Information for details).
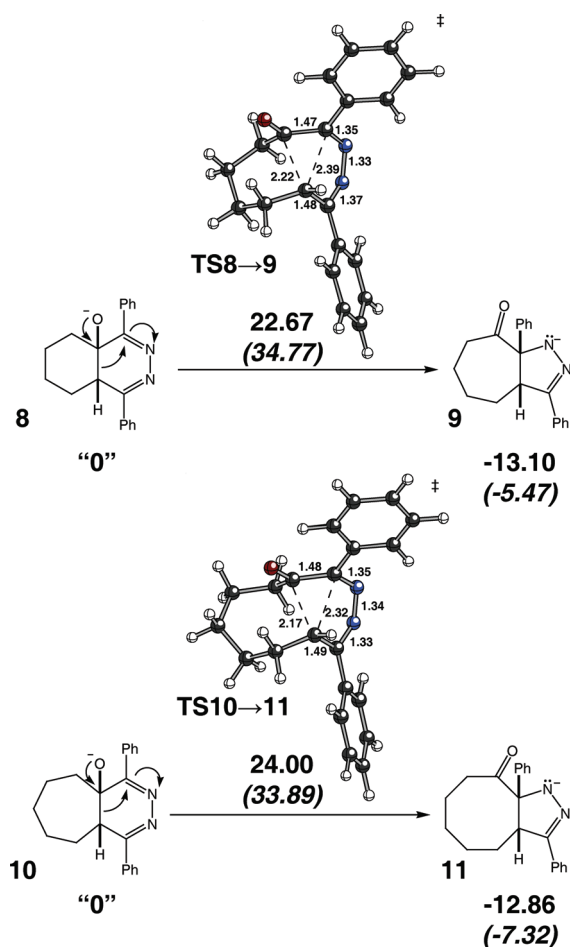
Evident from these data is the fact that the electrocyclic ring opening of the cyclobutanone-derived system is the only reaction that is both exergonic and proceeds via a low barrier (in solvent). This is not surprising considering the strain release associated with opening a four-membered ring, particularly one which would be fused to an aromatic ring if the pyridazine were formed. Among the ring-opening possibilities for the larger systems, the fragmentation pathway appears to become favored from a kinetic standpoint. It appears that, for the cyclooctanone-derived system, the pathway which leads to the formally forbidden conrotatory product is actually highly favored over the pathway leading to the orbital symmetry-allowed disrotatory product! This preference likely results from the relative difference in strain between the two transition-state structures, which is reflected to an even greater extent in the two products. Note in particular that, for the system derived from cyclobutanone, the electrocyclic product is over 20 kcal/mol lower in energy than the fragmentation product, while in the system derived from cyclooctanone, the two products are much closer in energy.[28]

Note also the entry for 2,2,6-trimethylcyclohexanone. This system was chosen such that intermediate **5** (Schemes 2 and 6) would be unable to undergo elimination to form the aromatic pyridazine product since it lacks the requisite proton.[29] Consequently, either the 1,2-shift to form a bicyclic pyrazoline (at high temperatures where the thermodynamic product is formed) or the ring opening to form a diazocinone (at low temperatures where the kinetic product is formed) should occur, unless intermediate **4′** is simply protonated to form a pyridazine derivative (Scheme 7).[30,31] All three of these possible products correspond to interesting heterocyclic systems.[31]

FIGURE 4. Computed energies (B3LYP/6-31+G(d,p)) and transition-state structures for oxyanion-accelerated [1s, 2s]-sigmatropic shifts leading to 7,5- and 8,5-fused ring systems. Energies are in kcal/mol; regular text shows gas-phase free energy values, italicized text in parentheses shows solvent single-point electronic energy values (see Methods). Selected distances are in Å.

(27) In general, synthesis of medium-sized rings tends to be relatively challenging. For reviews, see (a) Maier, M. E. *Angew. Chem., Int. Ed.* **2000**, *39*, 2073–2077. (b) Yet, L. *Chem. Rev.* **2000**, *100*, 2963–3007.

(28) The relative difference in energy here results in a fragmentation transition-state structure that is earlier than the competing electrocyclic process for the cyclooctanone derived system. See Supporting Information for these structures.

(29) This ketone was also chosen because it has only one α-proton and is synthetically accessible.

(30) The intermediate resulting from step (a) on the way to fused pyrazolines could potentially be protonated on the nitrogen (as shown) or on C8 to produce one of two possible diastereomeric products. Calculations on these possibilities for the system arising from 2,2,6-trimethylcyclohexanone reveal *N*-protonation to be thermodynamically favored over both *C*-protonation possibilities by approximately 11−16 kcal/mol.
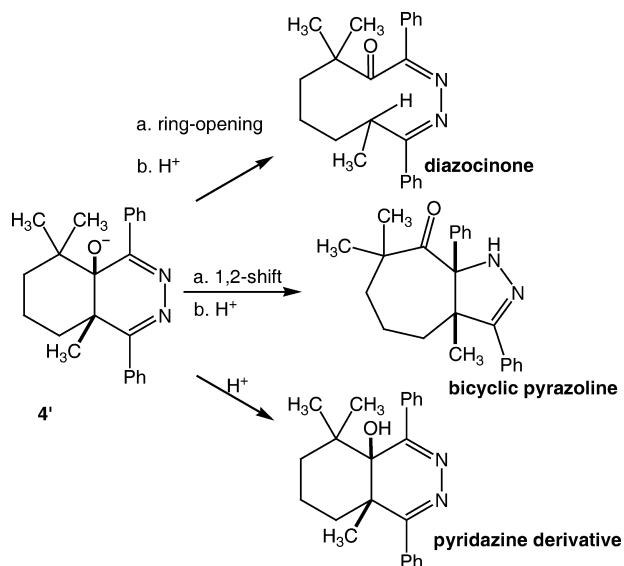
(31) (a) Pyrazoline derivatives have been shown to have interesting biological activities. For a recent example, see Frank, E.; Mucsi, Z.; Zupkó, I.; Réthy, B.; Falkay, G.; Schneider, G.; Wölfling, J. *J. Am. Chem. Soc.* **2009**, *131*, 3894–3904. Interestingly, pyrazoline derivatives have previously been found to result from the reaction of tetrazines with other enolate species, albeit through a different proposed mechanism. See (b) Suen, Y. F.; Hope, H.; Nantz, M. H.; Haddadin, M. J.; Kurth, M. J. *J. Org. Chem.* **2005**, *70*, 8468–8471. (c) Suen, Y. F.; Hope, H.; Nantz, M. H.; Haddadin, M. J.; Kurth, M. J. *Tetrahedron Lett.* **2006**, *47*, 7893–7896.

TABLE 2.   Ring-Opening Reactions for Cyclobutanone through Cyclooctanone Systems[a]

reactant ketone	allowed electrocyclic		1,2-shift		fragmentation	
	$\Delta E^{\ddagger}$	ΔE	$\Delta E^{\ddagger}$	ΔE	$\Delta E^{\ddagger}$	ΔE
cyclobutanone	9.64 *(18.14)*	−12.11 *(−0.67)*	−	−	22.76 *(33.38)*	10.21 *(21.44)*
cyclopentanone	11.43 *(21.69)*	4.93 *(17.34)*	−	−	20.54 *(31.86)*	13.36 *(25.97)*
cyclohexanone	−	−	22.67 *(34.77)*	−13.10 *(−5.47)*	15.33 *(25.22)*	10.08 *(21.09)*
2,2,6-trimethyl-cyclohexanone	−	−	22.34 *(32.61)*	−6.95 *(−4.55)*	15.79 *(21.91)*	11.82 *(17.42)*
cycloheptanone	−	−	24.00 *(33.89)*	−12.86 *(−7.32)*	13.40 *(22.22)*	8.08 *(18.77)*
cyclooctanone	23.76 *(33.11)*	−5.50 *(2.52)*	−	−	10.74 *(15.29)*	−1.33 *(4.96)*

[a] Energies (B3LYP/6-31+G(d,p)) are in kcal/mol; regular text shows gas-phase free energy values; italicized text in parentheses shows solvent single-point electronic energy values (see Methods).

SCHEME 7

For the key ring-opening step in these cascades, we uncovered theoretical evidence for two distinct processes: an allowed six-electron electrocyclic ring-opening reaction and a fragmentation process that displays some characteristics of a forbidden electrocyclic process. Our theoretical results suggest that ring opening likely occurs exclusively via the allowed electrocyclic process for most systems, although the formally forbidden ring opening is predicted to be favored for systems derived from cyclooctanone.

We also uncovered evidence in systems derived from cyclohexanone and cycloheptanone that an oxyanion-accelerated [1s, 2s]-sigmatropic shift, which although not yet observed experimentally, might occur for certain analogues where the prevailing pyridazine-forming elimination reaction is not an option. If borne out experimentally, this process would form unique fused pyrazoline systems. Experimental efforts toward this end are currently underway.

Supporting Information Available: Coordinates and energies for all structures, IRC plots, full GAUSSIAN citation, discussion of imaginary frequencies for **TS4 → 6** and **TS4 → 7** (and movie files), discussion of pyridazine-forming steps, and relaxed potential energy surface scans. This material is available free of charge via the Internet at http://pubs.acs.org.

JO900565Y

Conclusions

We have utilized a computational approach to study the many intricacies of the diazocinone and pyridazine-forming cascades that result from the reaction of tetrazines with cyclic enolate species. Many of the steps in these cascades can be formulated as oxyanion-accelerated pericyclic reactions. In examining these, we have uncovered several unexpected processes. In the initial stages of these cascades, we predict that a unique stepwise version of a formal (4 + 2) cycloaddition/(4 + 2) cycloreversion sequence occurs where a single C−C bond is formed in the first step. The remaining three bond-making/breaking events occur in a concerted but asynchronous fashion in the second step.